actuators

MDPI

Article

# Backstepping-Based Recursive Virtual-Heading Path-Tracking Control for Reverse Driving of a Multi-Trailer System

**Heeseok Shin [1,†], Myeongjun Kim [2,†], Heechang Moon [3] and Jeonghoon Kwak [4,*]**

1 Department of Intelligent Drone Convergence, Sejong University, Seoul 05006, Republic of Korea; hsshin9017@sejong.ac.kr
2 Department of Electrical and Control Engineering, Cheongju University, Cheongju 28503, Republic of Korea; kmjcr7@cju.ac.kr
3 Department of Mechanical and System Design Engineering, Hongik University, Seoul 04066, Republic of Korea; hcmoon@hongik.ac.kr
4 AI+X Research Center, Advanced Institute of Convergence Technology (AICT), Suwon 16229, Republic of Korea
* Correspondence: jeonghoon@snu.ac.kr
† These authors contributed equally to this work.

**Abstract**

Reverse path tracking of multi-trailer systems is challenging because tractor steering affects the following bodies only through passive hitch joints, causing tracking-error propagation and increasing the risk of jackknifing. This paper proposes a backstepping-based recursive virtual-heading (BS-RVH) controller that converts the path-tracking error of the final trailer into a desired heading rate and recursively generates the desired hitch angles, preceding-body heading rates, and tractor steering command. Desired hitch-angle saturation is included, and local boundedness and the effect of saturation residuals are analyzed. For a tractor–two-trailer system, BS-RVH achieves lateral root-mean-square errors of 0.015 m, 0.021 m, and 0.013 m on the S-curve, circular, and figure-eight paths, respectively. These values represent reductions of 93.0–93.4% compared with the curvature-based controller. The maximum absolute hitch angles remain below 12°, and all paths reach the predefined 99.5% completion threshold without jackknifing. An additional tractor–three-trailer evaluation completes the same paths without jackknifing, with lateral root-mean-square errors ranging from 0.073 m to 0.112 m. These results demonstrate the effectiveness and stage-wise extensibility of BS-RVH under low-speed kinematic conditions.

**Keywords:** multi-trailer system; reverse driving; path tracking; virtual heading; hitch-angle stabilization; jackknife prevention; autonomous vehicle

Check for updates

Academic Editors: Mohamed Reda, Ahmed Mahmoud Onsy and Ali Ghanbari

Received: 2 August 2026
Revised: 13 September 2026
Accepted: 16 September 2026
Published: 19 September 2026



## 1. Introduction

In last-mile logistics, port transportation, and confined-space maneuvering, a tractor connected to multiple passive trailers may be required to follow a prescribed path in reverse because sufficient turning space is unavailable. Stable reverse path tracking of such multi-trailer systems is therefore an important control problem for the practical deployment of autonomous logistics and transportation platforms.

In this paper, a multi-trailer system is defined as a tractor connected in series to two or more passive trailers. Let $N$ denote the number of trailers. The case $N = 1$ corresponds to a single-trailer system, whereas $N \geq 2$ involves multiple hitch connections and at least one intermediate passive body. The primary comparative evaluation in this study is conducted using $N = 2$, which represents the minimum multi-trailer configuration in which cascaded hitch dynamics arise. An additional $N = 3$ case is considered to examine the stage-wise extensibility of the proposed recursive structure.

Reverse control of a multi-trailer system is inherently unstable because steering actuation is available only at the tractor, while the motion of each following body is determined indirectly by the heading response of the preceding body through passive hitch joints. During reverse motion, heading-response delays and hitch-angle amplification can propagate along the hitch chain, causing even small tracking errors to develop into excessive articulation or jackknifing.

Early studies on single-trailer systems established fundamental control structures for reverse trajectory tracking, path following, and articulation stabilization. Pradalier and Usher addressed trajectory tracking for a tractor–trailer system [1], while Leng and Minor proposed a backing control law for reverse path following [2]. More recent studies have investigated nonlinear MPC, sliding-mode control, and path-following control under wheel-slip conditions, demonstrating the importance of accounting for kinematic uncertainty, actuator constraints, and articulation behavior in practical systems [3–5]. In reverse pure-pursuit control, the tractor heading can be interpreted as a virtual steering input to the trailer, and the tractor steering command can be calculated by considering the trailer length and hitch angle [6]. Although this virtual-steering interpretation provides a computationally efficient control structure for a single trailer, it does not explicitly represent the cascaded heading propagation occurring through multiple passive hitch joints.

At the broader nonlinear tracking-control level, backstepping, adaptive control, robust control, and predictive control have been developed to establish tracking-error convergence or boundedness under model uncertainties and disturbances. Hu and Ma proposed an adaptive event-triggered tracking controller using switching functions, command filtering, and adaptive backstepping to obtain finite-time stability for uncertain nonlinear systems [7]. Hu et al. developed a resilient memory-event-triggered predictive tracking controller for an unmanned ground vehicle and incorporated stability conditions into the MPC framework [8]. These studies demonstrate the importance of explicitly characterizing closed-loop stability and robustness. However, their control structures do not address the rear-to-front propagation of virtual heading commands through a chain of unactuated trailer bodies.

For multi-trailer systems, Cheng et al. presented a chained-dynamics-based method for backward orientation tracking of a mobile robot with $N$ trailers [9]. Kolb et al. analyzed the stability conditions of reverse path tracking for a system comprising $N$ passive trailers, while Lukassek et al. proposed an MPC method that enables a general $N$-trailer system to follow an arbitrary guidance point [10,11]. Bertolani et al. experimentally validated the reverse control of a multi-articulated robot with one- and two-trailer configurations, and their subsequent work addressed jackknife risk and obstacle avoidance using gain modulation and null-space-based control [12,13].

Morales et al. interpreted the last trailer as a virtual tractor and recursively calculated reverse-curvature limits from the geometric constraints of multiple hitch joints [14]. Zhao et al. transformed desired-curvature tracking for $N$ on-axle trailers into a reference articulation-angle stabilization problem and analyzed the closed-loop stability of the resulting cascade structure [15]. Nonlinear optimal control, robust control, and model predictive path following have also been investigated for generalized multi-trailer systems subject to disturbances, sensor noise, and model uncertainty [16–18]. Lukassek et al. further demonstrated the real-time feasibility of path-following MPC using a scaled platform with up to two trailers [19].

https://doi.org/10.3390/act15090493

Existing multi-trailer studies have primarily addressed orientation stabilization, curvature constraints, robust control, or optimization-based path following. These approaches provide important stability and constraint-handling foundations, but relatively little attention has been given to a computationally efficient recursive structure that directly converts the path-tracking error of the final trailer into the desired hitch angle and desired heading rate of each preceding body. In particular, a stage-wise rear-to-front formulation is needed to represent explicitly how the motion requirement of the final tracking body is transmitted through intermediate passive bodies to the tractor steering actuator.

In a tractor–two-trailer system, the heading of trailer 1 acts as a virtual steering input to trailer 2, while the tractor heading acts as a virtual steering input to trailer 1. Consequently, the desired motions of the intermediate trailer and tractor must be determined sequentially to produce the required motion of the final trailer. To account for this cascaded relationship, this paper proposes a backstepping-based recursive virtual-heading (BS-RVH) path-tracking controller. The proposed controller converts the lateral and heading errors of the final trailer into a desired heading rate and recursively propagates the resulting virtual-control commands from rear to front through the passive hitch chain. At each recursive stage, a desired hitch angle and the desired heading rate of the preceding body are generated, ultimately producing the tractor steering command.

Desired hitch-angle saturation is incorporated to constrain the recursively generated commands. Because saturation modifies the nominal virtual control, its residual is explicitly formulated as a bounded disturbance transmitted to the subsequent recursive stage. A Lyapunov-based local analysis is also provided to establish conditions for convergence or ultimate boundedness of the hitch-angle and path-tracking errors under the low-speed kinematic assumptions considered in this study.

The primary evaluation is conducted using a tractor connected to two passive on-axle trailers. DSE, CURV, and BS-RVH are compared on S-curve, circular, and figure-eight paths using the same plant model, initial conditions, reverse velocity, sampling time, steering constraints, and termination criteria. In addition, a tractor–three-trailer system is evaluated on the same path types to examine recursive error propagation, command saturation, and the stage-wise scalability of BS-RVH.

The main contributions of this study are summarized as follows.

- A backstepping-based recursive virtual-heading structure is proposed to account explicitly for heading propagation through intermediate passive bodies and interactions among multiple hitch joints during reverse path tracking.
- A general stage-wise control relation is formulated to recursively generate the desired hitch angle and desired heading rate of each preceding body from the path-tracking error of the final trailer, ultimately producing the tractor steering command.
- A Lyapunov-based local stability analysis is provided to establish conditions for convergence or ultimate boundedness of the path-tracking and hitch-angle errors. The effect of desired hitch-angle saturation is represented as a bounded residual propagated through the recursive stages.
- DSE, CURV, and BS-RVH are quantitatively compared under common plant, motion, steering, and termination conditions on S-curve, circular, and figure-eight paths. The controller-tuning procedure and parameter effects are also clarified to support a fair comparison.
- The proposed recursive structure is extended to a tractor–three-trailer system. The additional evaluation examines the tracking error, articulation response, command saturation, and path-completion performance of the extended hitch chain.

https://doi.org/10.3390/act15090493

# 2. Methodology

## *2.1. Multi-Trailer System Configuration*

A general multi-trailer system is defined as a tractor connected in series to $N$ passive trailers. The primary controller design and comparative evaluation in this study consider $N = 2$, which is the minimum multi-trailer configuration containing an intermediate passive body and two cascaded hitch joints. The tractor, first trailer, and second trailer are denoted as body 0, body 1, and body 2, respectively. The steering input is applied only to the tractor, while the trailers are passive bodies connected through on-axle hitch joints. An additional $N = 3$ configuration is evaluated in Section 4.4 to examine the stage-wise extensibility of the proposed structure.

In the $N = 2$ configuration, body 1 acts as the intermediate body and body 2 is the final path-tracking body. Therefore, the desired motions of body 1 and body 0 must be generated sequentially from the path-tracking error of body 2. This rear-to-front heading propagation constitutes the basic principle of the proposed recursive virtual-heading structure.

Figure 1 illustrates the geometric configuration of the tractor–two-trailer system. The coordinates of the trailers are defined at their axle centers, while $(x_0, y_0)$ denotes the rear-axle center of the tractor rather than its center of gravity. This coordinate is consistent with the kinematic bicycle model and the assumed on-axle hitch configuration. It allows the tractor heading rate to be expressed without an additional center-of-gravity offset or sideslip term and provides a direct geometric connection to trailer 1.

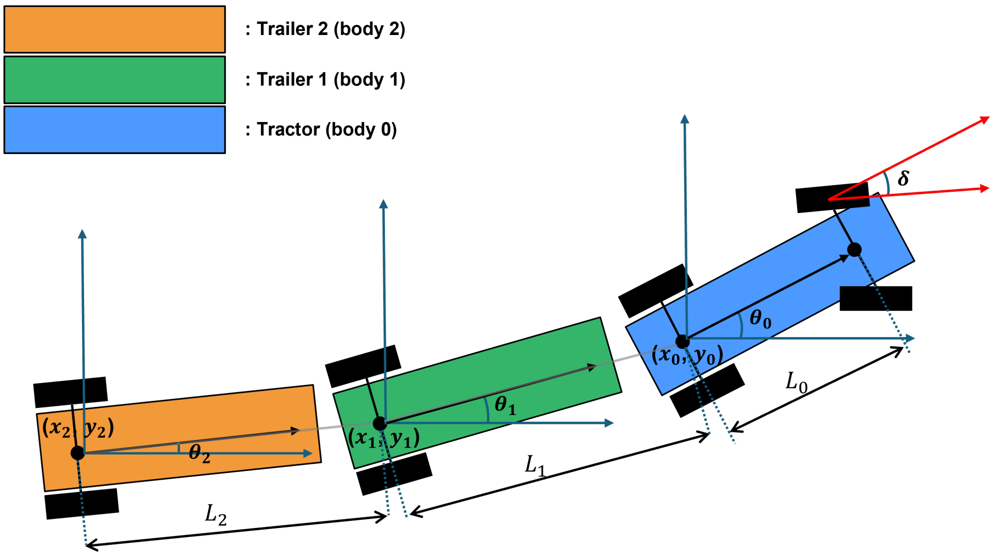


**Figure 1.** Geometric configuration and notation of the tractor–two-trailer system. Body 0 denotes the tractor, while body 1 and body 2 denote the first and second passive trailers, respectively.

The state variables and system parameters are defined as follows.

- $(x_i, y_i)$: axle-center position of body $i$, with $(x_0, y_0)$ defined at the tractor rear-axle center;
- $\theta_i$: heading angle of body $i$;
- $\psi_1 = \text{wrap}(\theta_0 - \theta_1)$: hitch angle between the tractor and trailer 1;
- $\psi_2 = \text{wrap}(\theta_1 - \theta_2)$: hitch angle between trailer 1 and trailer 2;
- $\delta$: tractor steering angle;
- $v_i$: signed longitudinal velocity of body $i$;
- $L_0$: tractor wheelbase;
- $L_1$: distance from the first hitch joint to the axle center of trailer 1;
- $L_2$: distance from the second hitch joint to the axle center of trailer 2.

Here, $i = 0, 1, 2$ denotes the tractor, trailer 1, and trailer 2, respectively. All heading and hitch angles are normalized to $[-\pi, \pi]$ using

$$\mathrm{wrap}(\theta) = \mathrm{atan2}(\sin\theta, \cos\theta). \tag{1}$$

*2.2. Chained Kinematic Model*

An on-axle configuration is assumed in which each hitch joint is located at the rear-axle center of the preceding body. The purpose of this study is to investigate the recursive geometric heading propagation and hitch-angle regulation mechanism during low-speed reverse motion. Accordingly, a kinematic model is adopted to isolate the proposed rear-to-front virtual-heading control structure from additional dynamic effects. The nominal simulations use a constant reverse speed of 0.40 m/s, for which the nonholonomic no-slip constraints provide the geometric relation between tractor steering, hitch angles, and trailer motion.

Tire slip, suspension compliance, hitch backlash, steering-actuator dynamics, and dynamic load transfer can influence practical transient responses; however, they are outside the scope of the present nominal kinematic validation. The present study therefore does not claim dynamic robustness. These effects are identified as the next validation stage using high-fidelity dynamic simulation and physical experiments.

The variables $v_0$, $v_1$, and $v_2$ denote the signed longitudinal velocities along the corresponding body axes, and $v_0 < 0$ during reverse motion. The tractor kinematics are

$$\dot{x}_0 = v_0 \cos\theta_0, \tag{2}$$
$$\dot{y}_0 = v_0 \sin\theta_0, \tag{3}$$
$$\dot{\theta}_0 = \frac{v_0}{L_0} \tan\delta. \tag{4}$$

According to the on-axle kinematic constraints, the longitudinal velocities of trailer 1 and trailer 2 are propagated as

$$v_1 = v_0 \cos\psi_1, \tag{5}$$
$$v_2 = v_1 \cos\psi_2 = v_0 \cos\psi_1 \cos\psi_2. \tag{6}$$

The heading rates of the trailers are given by

$$\dot{\theta}_1 = \frac{v_0}{L_1} \sin\psi_1, \tag{7}$$
$$\dot{\theta}_2 = \frac{v_1}{L_2} \sin\psi_2 = \frac{v_0 \cos\psi_1}{L_2} \sin\psi_2. \tag{8}$$

The trailer positions and hitch angles evolve according to

$$\dot{x}_i = v_i \cos\theta_i, \qquad i \in \{1, 2\}, \tag{9}$$
$$\dot{y}_i = v_i \sin\theta_i, \qquad i \in \{1, 2\}, \tag{10}$$
$$\dot{\psi}_1 = \dot{\theta}_0 - \dot{\theta}_1, \tag{11}$$
$$\dot{\psi}_2 = \dot{\theta}_1 - \dot{\theta}_2. \tag{12}$$

*2.3. Backstepping-Based Recursive Virtual-Heading Control*

The proposed BS-RVH controller converts the path-tracking error of the final trailer into a desired heading rate and propagates the resulting virtual-control commands from rear to front through the passive hitch chain. At time step $k$, let $j_k$ denote the index of the reference-path point associated with trailer 2. The position and tangent direction at that point are denoted by $\boldsymbol{p}_{j_k}$ and $\theta_{\text{ref}}(j_k)$, respectively.

The reference-path normal vector and signed lateral error of trailer 2 are defined as

$$\boldsymbol{n}_{j_k} = \begin{bmatrix} -\sin\theta_{\text{ref}}(j_k) \\ \cos\theta_{\text{ref}}(j_k) \end{bmatrix}, \qquad e_y(k) = \boldsymbol{n}_{j_k}^{\top}\left(\boldsymbol{p}_2(k) - \boldsymbol{p}_{j_k}\right). \tag{13}$$

During reverse motion, the travel heading and heading error of trailer 2 are defined as

$$\beta_2(k) = \text{wrap}(\theta_2(k) + \pi), \qquad e_\theta(k) = \text{wrap}(\theta_{\text{ref}}(j_k) - \beta_2(k)). \tag{14}$$

The corrected heading error is defined as

$$e_h(k) = \text{wrap}\left[e_\theta(k) - \arctan\left(\frac{K_{\text{ct}} e_y(k)}{K_{\text{soft}} + |v_0|}\right)\right]. \tag{15}$$

The desired heading rate of trailer 2 is generated as

$$\dot{\theta}_{2,d}(k) = K_{\text{head}} e_h(k). \tag{16}$$

For a general $N$-trailer system, the heading kinematics of body $i$ are given by $\dot{\theta}_i = [v_{i-1}/L_i]\sin\psi_i$. Once the desired heading rate of body $N$ is specified, the desired hitch-angle command and desired heading rate of the preceding body at each hitch stage can be calculated recursively as

$$\begin{aligned} \psi_{i,d}(k) &= \arcsin\left[\text{sat}\left(\frac{L_i \dot{\theta}_{i,d}(k)}{v_{i-1}(k)}, -\sin\psi_{i,\max}, \sin\psi_{i,\max}\right)\right], \\ e_{\psi_i}(k) &= \text{wrap}(\psi_{i,d}(k) - \psi_i(k)), \\ \dot{\theta}_{i-1,d}(k) &= \dot{\theta}_i(k) + K_{\psi_i} e_{\psi_i}(k), \qquad i = N, N-1, \ldots, 1. \end{aligned} \tag{17}$$

In this study, the primary comparative evaluation applies Equation (17) to a tractor–two-trailer system with $N = 2$. Accordingly, $\psi_{2,d}$, $\dot{\theta}_{1,d}$, $\psi_{1,d}$, and $\dot{\theta}_{0,d}$ are calculated sequentially from $\dot{\theta}_{2,d}$.

By inverting the tractor kinematics and applying the steering-angle limit, the BS-RVH steering command is obtained as

$$\delta_{\text{BS-RVH}}(k) = \arctan\left[\text{sat}\left(\frac{L_0 \dot{\theta}_{0,d}(k)}{v_0(k)}, -\tan\delta_{\max}, \tan\delta_{\max}\right)\right]. \tag{18}$$

The same stage-wise recursive relation is subsequently extended to a tractor–three-trailer system by adding one recursive hitch-control stage. The control flow and the general rear-to-front propagation procedure are illustrated in Figure 2. The local boundedness properties and the effect of desired hitch-angle saturation are analyzed in the following subsection. The analysis is restricted to the stated low-speed kinematic operating region and does not claim global closed-loop stability over the entire state space.

### 2.4. Algorithmic Procedure

Figure 2 presents the BS-RVH algorithmic procedure. At each sampling instant, the reference path and the terminal-trailer state are used to calculate the lateral and travel-heading errors. The corrected heading error generates the desired heading rate of the terminal trailer. The recursive block is then evaluated from $i = N$ to $i = 1$ to calculate the feasible desired hitch angle and the desired heading rate of each preceding body. Finally, the desired tractor heading rate is converted into an Ackermann steering command, subject to steering-angle and steering-rate constraints, and the chained kinematic model updates the system state for the next sampling instant.

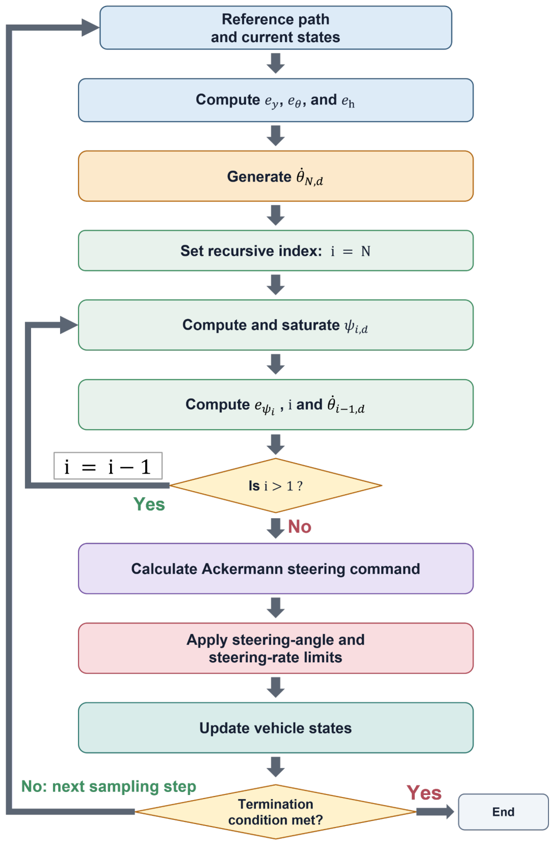


**Figure 2.** Flowchart of the proposed BS-RVH control algorithm.

### *2.5. Local Boundedness and Saturation Effects*

The following analysis considers a local constant-speed operating region satisfying $|v_{i-1}| \geq v_{\min} > 0$ and $|\psi_i|, |\psi_{i,d}| \leq \psi_{i,\max} < \pi/2$. The desired-command derivatives and interstage heading-rate mismatches are assumed to be bounded.

Define the hitch-angle error and the preceding-body heading-rate mismatch as

$$e_{\psi_i} = \mathrm{wrap}(\psi_{i,d} - \psi_i), \qquad d_{i-1} = \dot{\theta}_{i-1,d} - \dot{\theta}_{i-1}. \tag{19}$$

Using $\dot{\psi}_i = \dot{\theta}_{i-1} - \dot{\theta}_i$ and Equation (17), the local hitch-angle error dynamics are

$$\dot{e}_{\psi_i} = -K_{\psi_i} e_{\psi_i} + \dot{\psi}_{i,d} + d_{i-1}. \tag{20}$$

For $V_i = e_{\psi_i}^2/2$,

$$\dot{V}_i \leq -K_{\psi_i} e_{\psi_i}^2 + |e_{\psi_i}|(|\dot{\psi}_{i,d}| + |d_{i-1}|). \tag{21}$$

Therefore, if $|\dot{\psi}_{i,d}| + |d_{i-1}| \leq \bar{\omega}_i$ and $K_{\psi_i} > 0$,

$$\limsup_{t\to\infty} |e_{\psi_i}(t)| \leq \frac{\bar{\omega}_i}{K_{\psi_i}}. \tag{22}$$

Hence, each recursive hitch-angle error is locally ultimately bounded and converges to zero when the command derivative and interstage mismatch vanish.

For the terminal-trailer tracking loop, let $u_N = |v_N| > 0$ and $c = K_{ct}/(K_{soft} + |v_0|) > 0$. For small errors on a straight path, the linearized homogeneous tracking-error system has the characteristic polynomial

$$\lambda^2 + K_{head}\lambda + u_N K_{head} c. \tag{23}$$

It is Hurwitz for $K_{head} > 0$, $u_N > 0$, and $c > 0$. Thus, the terminal-trailer tracking errors converge locally when the heading-rate mismatch vanishes and remain bounded under bounded curvature and interstage mismatch.

The saturation effect is represented by

$$z_i = \frac{L_i \dot{\theta}_{i,d}}{v_{i-1}}, \tag{24}$$

$$\bar{z}_i = \mathrm{sat}(z_i, -\sin\psi_{i,\max}, \sin\psi_{i,\max}), \tag{25}$$

$$d_{i,sat} = \dot{\theta}_{i,d} - \frac{v_{i-1}}{L_i}\bar{z}_i = \frac{v_{i-1}}{L_i}(z_i - \bar{z}_i). \tag{26}$$

The residual $d_{i,sat}$ is zero when the desired virtual command is feasible and acts as a bounded disturbance otherwise. Accordingly, the analysis establishes local boundedness under the stated assumptions, rather than global closed-loop stability.

## 3. Simulation

### *3.1. Comparison Controllers*

To evaluate the relative performance of the proposed BS-RVH controller, a direct single-trailer extension (DSE) and a curvature-based two-stage controller (CURV) were implemented as comparison controllers. DSE combines the heading difference between the tractor and trailer 2 into a single equivalent virtual hitch angle and does not employ a separate backstepping stage for trailer 1. CURV generates the desired curvature of trailer 2 from the reference-path curvature, lateral error, and corrected heading error, and subsequently calculates the tractor steering command through an articulation-stabilization stage [15]. In contrast, BS-RVH handles the hitch-angle errors of trailer 2 and trailer 1 in separate backstepping stages, as described in Section 2.3. The same multi-trailer plant model, reference paths, initial conditions, reverse velocity, and steering constraints were applied to all controllers.

### *3.2. Common Steering Constraints and Numerical Update*

The same steering-angle and steering-rate limits were applied to all controllers to ensure a fair comparison. Let $\delta_{cmd}(k)$ denote the steering command generated by DSE, CURV, or BS-RVH at time step $k$. The saturation function is defined as

$$\mathrm{sat}(z, a, b) = \min(\max(z, a), b), \tag{27}$$

where $z$ is the input and $a$ and $b$ are its lower and upper bounds, respectively.

A common final steering constraint was applied to the command of every controller. The command was first limited by the maximum steering-angle magnitude $\delta_{max}$. The change from the steering angle applied at the previous time step, $\delta(k-1)$, was then limited by the maximum steering rate $\dot{\delta}_{max}$. Accordingly, the steering angle applied at time step $k$ was calculated as

$$\begin{aligned} \delta_{lim}(k) &= \mathrm{sat}(\delta_{cmd}(k), -\delta_{max}, \delta_{max}), \\ \delta(k) &= \delta(k-1) + \mathrm{sat}\big(\delta_{lim}(k) - \delta(k-1), -\dot{\delta}_{max}\Delta t, \dot{\delta}_{max}\Delta t\big). \end{aligned} \tag{28}$$

Here, $\delta_{\text{lim}}(k)$ is the steering command after applying the steering-angle constraint, $\delta(k)$ is the steering angle ultimately applied to the tractor, $\dot{\delta}_{\text{max}}$ is the maximum steering-rate magnitude, and $\Delta t$ is the numerical integration time step. Thus, the maximum allowable steering-angle change during one integration step is $\dot{\delta}_{\text{max}}\Delta t$.

The applied steering angle $\delta(k)$ was used in the chained kinematic model. The tractor position and the body heading angles were advanced using an explicit Euler update. Subsequently, the trailer axle-center positions were reconstructed sequentially from the updated preceding-body positions and trailer headings. This numerical projection preserves the rigid hitch-to-axle distances $L_1$ and $L_2$ at every integration step.

*3.3. Simulation Setup*

The simulations were conducted under constant low-speed reverse-motion conditions, with trailer 2 designated as the final path-tracking body for all controllers. The same vehicle parameters, sampling time, steering constraints, and termination criteria were applied to all controllers.

The tractor reverse velocity was prescribed as the constant value $v_0 = -0.40$ m/s; therefore, the commanded longitudinal acceleration was zero except at the initialization instant. The trailer longitudinal velocities followed the kinematic relations $v_1 = v_0 \cos\psi_1$ and $v_2 = v_0 \cos\psi_1 \cos\psi_2$. Accordingly, the simulations evaluate spatial path-following and articulation behavior under a fixed low-speed reverse maneuver rather than longitudinal speed-control performance.

DSE and CURV employed adaptive look-ahead scheduling to account for changes in local path curvature and hitch articulation. A curvature–articulation scheduling term was first bounded within [0.55, 1.35], after which a controller-specific multiplier was applied to obtain the final look-ahead distance. Higher local curvature reduced the preview distance to improve tracking responsiveness, whereas increasing articulation increased the preview distance to promote a smoother response. To prevent excessively short preview distances, the body-specific look-ahead distances were calculated as

$$L_{d,i}(k) = \max\left(L_{d,i}^{\min}, L_{d,i}^{\text{adp}}(k)\right), \tag{29}$$

where $L_{d,i}^{\text{adp}}(k)$ denotes the adaptively scheduled look-ahead distance for body $i$. DSE used $L_{d,0}$, $L_{d,1}$, and $L_{d,2}$ to generate virtual target motions for the tractor, trailer 1, and trailer 2, respectively. CURV used $L_{d,2}$ to calculate the curvature-based tracking correction of trailer 2. In contrast, BS-RVH did not use a look-ahead distance because its desired heading rate was generated directly from the signed lateral error and corrected heading error at the reference-path point associated with trailer 2.

The vehicle parameters, controller-specific look-ahead parameters, steering constraints, and simulation termination parameters are listed in Table 1.

The parameters $L_0$, $L_1$, and $L_2$ denote the tractor wheelbase and the hitch-to-axle lengths of trailer 1 and trailer 2, respectively. The negative sign of $v_0$ indicates reverse motion, and $\Delta t$ is the numerical integration time step. The parameters $\delta_{\text{max}}$ and $\dot{\delta}_{\text{max}}$ define the steering-angle and steering-rate constraints applied to all controllers. The limits $\psi_{1,\text{max}}$ and $\psi_{2,\text{max}}$ constrain the desired hitch-angle commands and are distinct from the jackknife threshold $\psi_{\text{jk}}$. Finally, $C_{\text{succ}}$ and $T_{\text{max}}$ define the path-completion and maximum-time termination conditions, respectively.

The controller gains were selected according to their roles in the corresponding control laws. For DSE, $K_{\text{DSE}}$ is the proportional feedback gain that converts the equivalent virtual hitch-angle error into the tractor steering command. For CURV, $K_e$ and $K_h$ weight the lateral-error and corrected-heading-error terms, respectively, when generating the desired curvature of trailer 2, while $\kappa_{max}$ limits the magnitude of the curvature command. For BS-RVH, $K_{ct}$ scales the contribution of the signed lateral error to the corrected heading error, and $K_{soft}$ prevents excessive path-error correction at low longitudinal speeds. The gain $K_{head}$ converts the corrected heading error into the desired heading rate of trailer 2, whereas $K_{\psi_2}$ and $K_{\psi_1}$ determine the correction rates of the second and first hitch-angle errors in the recursive backstepping stages, respectively.

**Table 1.** Vehicle, controller-specific look-ahead, and simulation parameters used in the reverse-driving simulations.

| Parameter | Symbol | Value |
|---|---|---|
| Tractor wheelbase | $L_0$ | 2.65 m |
| First trailer hitch-to-axle length | $L_1$ | 2.50 m |
| Second trailer hitch-to-axle length | $L_2$ | 2.50 m |
| Tractor reverse velocity | $v_0$ | −0.40 m/s |
| Sampling time | $\Delta t$ | 0.02 s |
| Maximum steering-angle magnitude | $\delta_{max}$ | 35° |
| Maximum steering-rate magnitude | $\dot{\delta}_{max}$ | 110°/s |
| Maximum first hitch-angle command | $\psi_{1,max}$ | 70° |
| Maximum second hitch-angle command | $\psi_{2,max}$ | 70° |
| Jackknife threshold | $\psi_{jk}$ | 90° |
| Bounded curvature–articulation scheduling term (DSE and CURV only) | $\lambda_d$ | [0.55, 1.35] |
| Minimum tractor look-ahead distance (DSE only) | $L_{d,0}^{min}$ | 2.0 m |
| Minimum trailer 1 look-ahead distance (DSE only) | $L_{d,1}^{min}$ | 2.3 m |
| Minimum trailer 2 look-ahead distance (DSE and CURV only) | $L_{d,2}^{min}$ | 2.8 m |
| Completion threshold | $C_{succ}$ | 99.5% |
| Maximum simulation time | $T_{max}$ | Path-dependent, up to 1300 s |

The controller parameters were selected through a common offline tuning procedure. First, the steering-angle, steering-rate, vehicle-geometry, reverse-speed, and termination constraints were fixed identically for all controllers. Next, each controller was tuned using the same S-curve, circular, and figure-eight path set to obtain stable completion without path-specific retuning. The final parameter set was then fixed for all reported evaluations.

The gains were fixed at $K_{DSE} = 1.00$, $K_e = 0.30\ m^{-1}$, $K_h = 0.24\ m^{-1}$, $K_{ct} = 1.00\ s^{-1}$, $K_{soft} = 0.50$ m/s, $K_{head} = 1.00\ s^{-1}$, $K_{\psi_2} = 1.00\ s^{-1}$, and $K_{\psi_1} = 2.00\ s^{-1}$. The curvature-command bound of CURV was set to $\kappa_{max} = 0.376\ m^{-1}$. All gains and command bounds were maintained across the complete set of reference paths.

Each simulation was terminated when the path completion ratio reached $C_{succ} = 99.5\%$, either hitch angle crossed the jackknife threshold $\psi_{jk} = 90°$, or the simulation time reached $T_{max}$. The value of $T_{max}$ was selected according to the arc length of each reference path, with a maximum value of 1300 s. The completion threshold of 99.5% was introduced as a terminal tolerance to reduce discretization and reference-point selection effects near the endpoint of the reference path. A simulation was classified as successfully completed when $C_{path} \geq C_{succ}$ without jackknifing.

### 3.4. Evaluation Metrics

Controller performance was evaluated using the lateral root-mean-square error (RMSE) of trailer 2, maximum absolute hitch angles, path completion ratio, and occurrence of jackknifing. Because the sign of the lateral error $e_y(k)$ indicates only the side of the reference path on which trailer 2 is located, tracking performance was evaluated based on the error magnitude rather than its sign.

https://doi.org/10.3390/act15090493

Let $N_s$ denote the number of samples collected before simulation termination. The principal evaluation metrics were calculated as

$$\begin{aligned} \mathrm{RMSE}_y &= \sqrt{\frac{1}{N_s}\sum_{k=1}^{N_s} e_y^2(k)}, \\ |\psi_i|_{\max} &= \max_{1\le k\le N_s} |\psi_i(k)|, \qquad i \in \{1,2\}, \\ C_{\text{path}} &= \frac{s(j_{N_s})}{s(N_p)} \times 100\ [\%]. \end{aligned} \tag{30}$$

Here, $s(j_{N_s})$ and $s(N_p)$ denote the cumulative arc length up to the reference-path point corresponding to the terminal state and the total arc length of the reference path, respectively. Jackknifing was detected when either hitch angle crossed the prescribed threshold $\psi_{\text{jk}} = 90^\circ$ between two consecutive integration steps. Therefore, the maximum absolute hitch angle reported from the stored pre-termination samples may be slightly below 90°. A simulation was classified as successfully completed when $C_{\text{path}} \geq C_{\text{succ}}$ without jackknifing.

## 4. Results

### *4.1. Spatial Path-Tracking Results*

Figures 3–6 present the path-tracking results on the straight, S-curve, circular, and figure-eight paths, respectively. The straight path was used to verify the basic operation of the reverse kinematic model and controller implementations, while the three curved paths were used to compare controller performance.

On the straight path, DSE, CURV, and BS-RVH maintained trailer 2 near the reference path without a noticeable increase in articulation. In contrast, the S-curve, circular, and figure-eight paths required continuous steering and hitch-angle transitions, resulting in clear performance differences among the controllers.

CURV and BS-RVH successfully completed all three curved paths without jackknifing. In contrast, DSE exhibited an increasing second hitch angle and a corresponding increase in the path-tracking error of trailer 2, eventually causing the simulations to terminate according to the jackknife criterion. This difference was particularly evident on the figure-eight path, where the direction of curvature changed repeatedly.

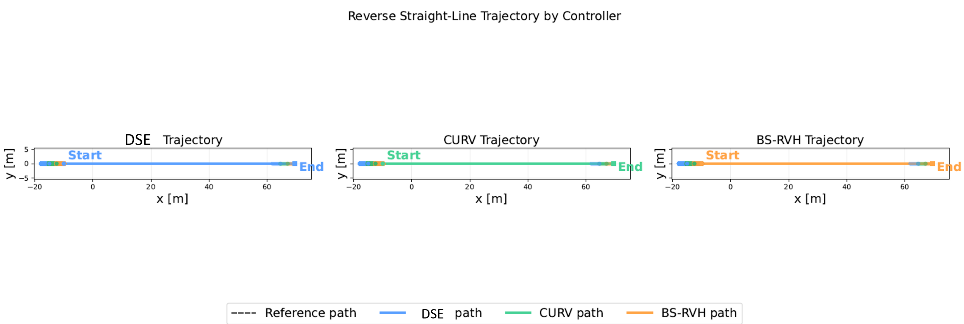


**Figure 3.** Path-tracking results of DSE, CURV, and BS-RVH on the straight reference path. The labels “Start” and “End” indicate the initial and final positions of trailer 2, respectively.

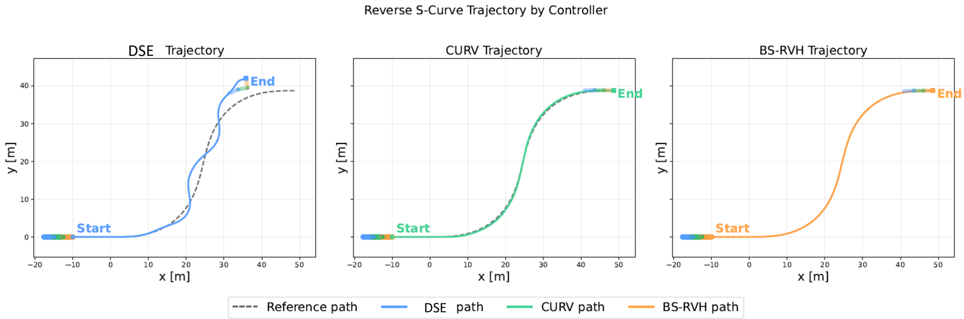


**Figure 4.** Path-tracking results of DSE, CURV, and BS-RVH on the S-curve reference path.

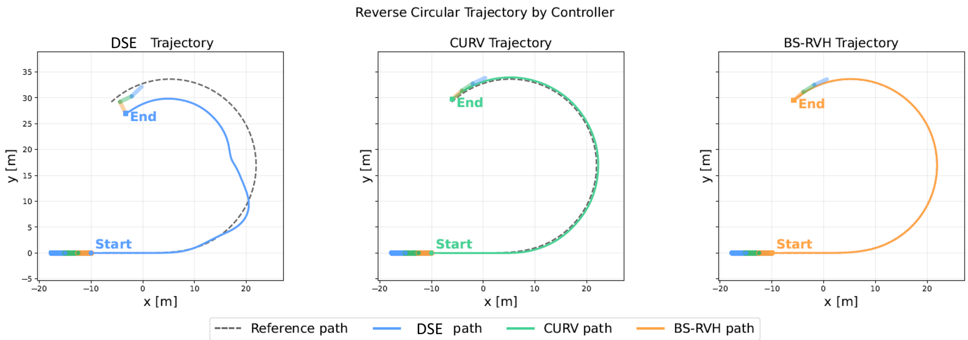


**Figure 5.** Path-tracking results of DSE, CURV, and BS-RVH on the circular reference path.

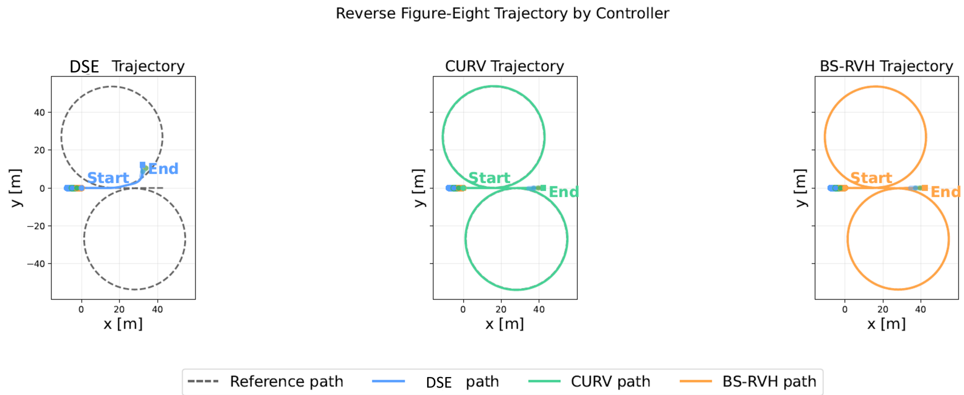


**Figure 6.** Path-tracking results of DSE, CURV, and BS-RVH on the figure-eight reference path. The controller results are presented in separate panels to improve visibility near the crossover.

### *4.2. Longitudinal Motion Response*

Figure 7 presents the signed body-axis velocities, hitch-angle responses, and derived longitudinal accelerations of the tractor and trailers under BS-RVH on the figure-eight path.

The tractor velocity was prescribed as $v_0 = -0.40$ m/s, and its longitudinal acceleration was zero throughout the maneuver. The trailer velocities were calculated from the no-slip kinematic relations $v_1 = v_0 \cos\psi_1$ and $v_2 = v_0 \cos\psi_1 \cos\psi_2$. Because the bodies have different orientations during turning, their axle-center body-axis velocities differ from the tractor velocity. Trailer 1 and trailer 2 velocities remained within $[-0.400, -0.3968]$ m/s and $[-0.400, -0.3953]$ m/s, respectively.

The derived longitudinal accelerations remained within $\pm 1.5 \times 10^{-3}$ m/s$^2$. The larger responses near 450 s and 900 s correspond to changes in reference-path curvature and the associated hitch-angle transients. The subsequent oscillations reflect the closed-loop articulation response within the kinematic model, while small residual ripples are associated with the finite spatial resolution of the reference path and discrete-time control updates.

These variations appear in the trailer velocities through the hitch-angle-dependent no-slip relations and are more apparent in their time derivatives. They should not be interpreted as physical vibration or force- and inertia-driven vehicle dynamics. Figure 7 therefore provides a kinematic description of the motion under the prescribed constant-speed condition, rather than dynamic validation.

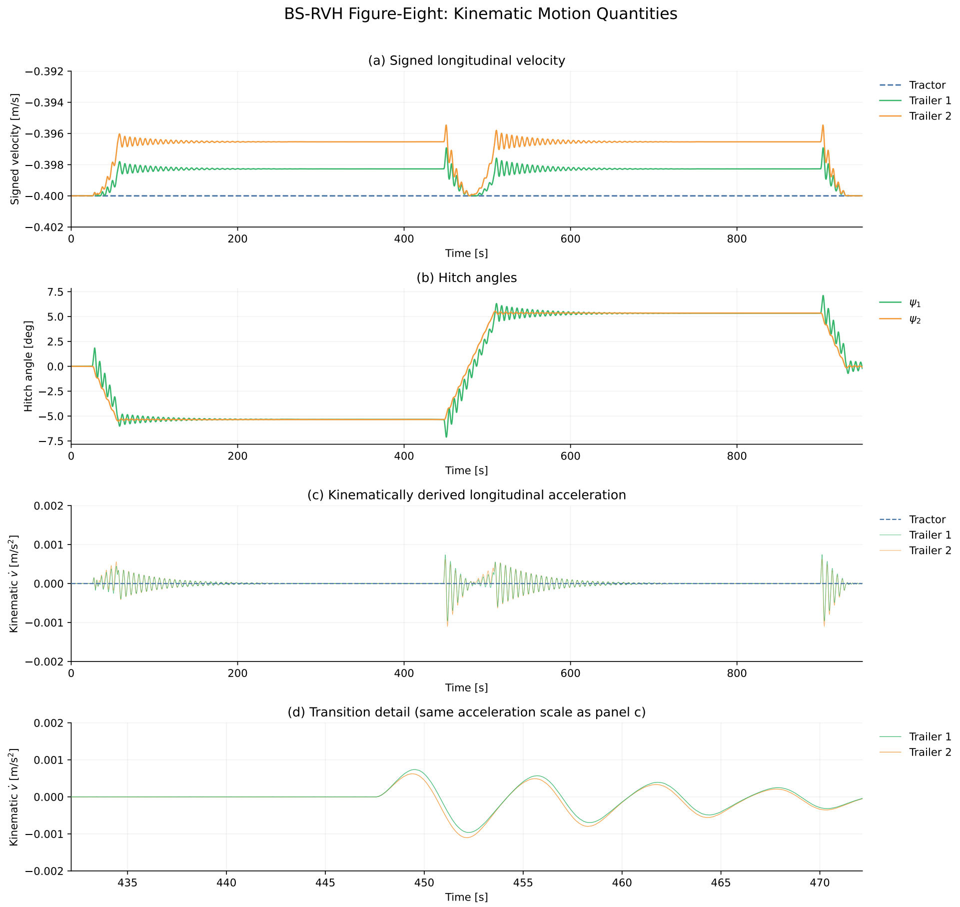


**Figure 7.** Kinematic velocity, hitch-angle, and longitudinal acceleration responses under BS-RVH on the figure-eight path. The accelerations represent body-axis velocity derivatives within the kinematic model.

### 4.3. Quantitative Tracking Results

Table 2 presents the quantitative performance comparison on the three curved paths. A simulation was classified as successfully completed when the path completion ratio reached or exceeded 99.5% without jackknifing. The straight-path results were excluded from the quantitative comparison because all three controllers operated without noticeable tracking errors or articulation growth.

Here, $|\psi_1|_{\max}$ denotes the maximum absolute hitch angle between the tractor and trailer 1, while $|\psi_2|_{\max}$ denotes that between trailer 1 and trailer 2 over the complete evaluation interval.

DSE achieved path completion ratios of 85.37%, 99.20%, and 10.08% on the S-curve, circular, and figure-eight paths, respectively. However, all three runs were classified as failed because $|\psi_2|$ approached the jackknife threshold of 90°. The completion ratio of 99.20% on the circular path does not indicate successful completion because jackknifing occurred immediately before the terminal completion criterion was satisfied.

**Table 2.** Quantitative comparison of reverse path-tracking performance. A run was classified as completed when the path completion ratio reached or exceeded 99.5% without jackknifing. A reported completion ratio of 99.50% indicates that this predefined threshold was successfully reached.

| Path | Method | RMSE$_y$ [m] | $\|\psi_1\|_{\max}$ [deg] | $\|\psi_2\|_{\max}$ [deg] | Jackknife | Completion [%] | Status |
|---|---|---|---|---|---|---|---|
| S-curve | DSE | 1.894 | 30.08 | 89.98 | Yes | 85.37 | Failed |
| | CURV | 0.226 | 10.81 | 10.06 | No | 99.50 | Completed |
| | BS-RVH | 0.015 | 9.63 | 8.82 | No | 99.50 | Completed |
| Circular | DSE | 2.853 | 27.85 | 89.97 | Yes | 99.20 | Failed |
| | CURV | 0.298 | 10.38 | 9.73 | No | 99.50 | Completed |
| | BS-RVH | 0.021 | 11.53 | 9.16 | No | 99.50 | Completed |
| Figure-eight | DSE | 1.454 | 29.76 | 89.95 | Yes | 10.08 | Failed |
| | CURV | 0.191 | 8.49 | 7.19 | No | 99.50 | Completed |
| | BS-RVH | 0.013 | 7.24 | 5.58 | No | 99.50 | Completed |

CURV successfully completed all three curved paths without jackknifing. The lateral RMSE values were 0.226 m, 0.298 m, and 0.191 m on the S-curve, circular, and figure-eight paths, respectively. The maximum absolute values of both hitch angles remained below 11° on all three paths.

BS-RVH achieved lateral RMSE values of 0.015 m, 0.021 m, and 0.013 m on the S-curve, circular, and figure-eight paths, respectively. Compared with CURV, these values correspond to reductions of 93.4%, 93.0%, and 93.2%, respectively. The value of $|\psi_2|_{\max}$ obtained by BS-RVH was smaller than that obtained by CURV on all three paths. However, $|\psi_1|_{\max}$ did not decrease consistently across all paths; on the circular path, BS-RVH and CURV produced values of 11.53° and 10.38°, respectively. Therefore, the principal quantitative advantage of BS-RVH should be interpreted as improved path-tracking accuracy of trailer 2 and regulation of the second hitch angle rather than a uniform reduction in both hitch angles.

In the nominal two-trailer simulations, the desired hitch-angle saturation was not activated on the S-curve, circular, or figure-eight paths. Therefore, the saturation residual defined in Equation (26) remained zero for the reported BS-RVH results. This indicates that the recursive virtual-heading commands remained within the prescribed feasible hitch-angle range under the evaluated nominal conditions.

### 4.4. Three-Trailer Scalability Validation

To examine the recursive extension of the proposed structure beyond the two-trailer comparison, an additional BS-RVH validation was conducted for a tractor–three-trailer system. The third trailer was designated as the final path-tracking body. The additional trailer length was set to $L_3 = 2.50$ m, while the steering-angle limit, steering-rate limit, hitch-angle command limit, and sampling time were maintained at the same values used in the two-trailer simulations. The reverse speed was set to $v_0 = -0.25$ m/s to provide a conservative low-speed operating condition for the longer articulated system.

Figure 8 presents the resulting trajectories on the straight, S-curve, circular, and figure-eight reference paths. The reference path and the trajectories of the tractor and all three trailers are shown separately to illustrate the rear-to-front propagation of the articulated motion.

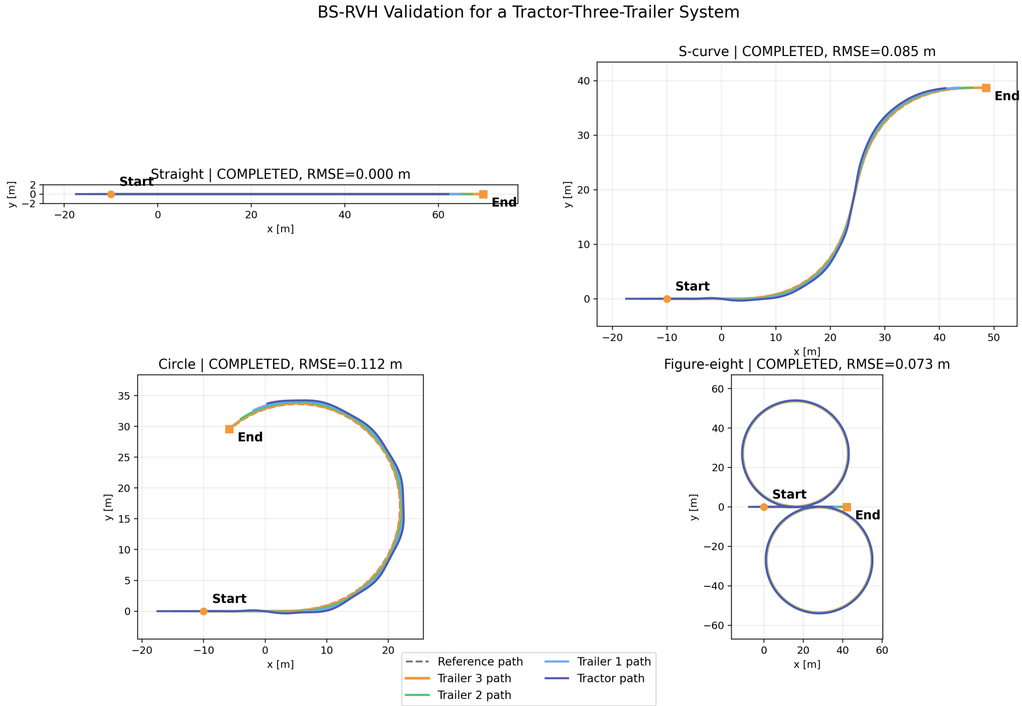


**Figure 8.** BS-RVH trajectory validation for a tractor–three-trailer system. The reference path and the trajectories of the tractor, trailer 1, trailer 2, and trailer 3 are shown for straight, S-curve, circular, and figure-eight paths. Trailer 3 is the final path-tracking body.

Table 3 summarizes the quantitative results. All four paths reached the predefined completion threshold without jackknifing. The straight-path result confirms the nominal equilibrium behavior of the extended kinematic chain. On the three curved paths, the lateral RMSE of trailer 3 remained below 0.12 m, while all hitch angles remained well below the 90° jackknife threshold.

**Table 3.** BS-RVH scalability validation for the tractor–three-trailer system. Trailer 3 was used as the final path-tracking body.

| Path | RMSE$_y$ [m] | $\lvert\psi_1\rvert_{max}$ [deg] | $\lvert\psi_2\rvert_{max}$ [deg] | $\lvert\psi_3\rvert_{max}$ [deg] | Completion [%] | Status |
|---|---|---|---|---|---|---|
| Straight | <0.001 | <0.001 | <0.001 | <0.001 | 99.50 | Completed |
| S-curve | 0.085 | 10.76 | 9.64 | 9.11 | 99.50 | Completed |
| Circular | 0.112 | 14.36 | 11.67 | 10.18 | 99.50 | Completed |
| Figure-eight | 0.073 | 9.46 | 7.42 | 6.39 | 99.50 | Completed |

The three-trailer BS-RVH controller achieved lateral RMSE values of 0.085 m, 0.112 m, and 0.073 m on the S-curve, circular, and figure-eight paths, respectively. On the figure-eight path, which requires repeated curvature reversals, the maximum hitch angles were 9.46°, 7.42°, and 6.39° for $\psi_1$, $\psi_2$, and $\psi_3$, respectively. The desired hitch-angle saturation was not activated in the nominal three-trailer validation cases, and the corresponding saturation residual remained zero.

These results demonstrate that the BS-RVH structure can incorporate an additional recursive stage for trailer 3 while maintaining bounded articulation and successful path completion under the nominal kinematic conditions considered in this study. The validation supports the stage-wise scalability of the recursive virtual-heading formulation, although systematic robustness analysis for larger numbers of trailers remains outside the scope of the present study.

## 5. Discussion

The results demonstrate the importance of explicitly accounting for heading propagation through the intermediate passive body during reverse path tracking of a multi-trailer system. DSE combines the heading difference between the tractor and trailer 2 into a single equivalent virtual hitch angle and does not regulate the two hitch-angle errors through separate recursive stages. Consequently, $|\psi_2|$ increased toward the jackknife threshold on the S-curve, circular, and figure-eight paths, and all DSE simulations were terminated according to the jackknife criterion.

CURV generated the desired curvature of trailer 2 from the reference-path curvature, lateral error, and corrected heading error, and subsequently converted this target motion into a tractor steering command through an articulation-stabilization stage. CURV reached the predefined path-completion threshold of 99.5% on all three curved paths without jackknifing. These results indicate that the curvature-based two-stage structure is effective for reverse multi-trailer path tracking under the nominal kinematic conditions considered in this study.

The proposed BS-RVH controller converts the corrected heading error of trailer 2 into a desired heading rate and recursively propagates this command through the desired hitch angles and heading rates of the preceding bodies. BS-RVH achieved lateral RMSE values of 0.015 m, 0.021 m, and 0.013 m on the S-curve, circular, and figure-eight paths, respectively. Compared with the corresponding CURV values of 0.226 m, 0.298 m, and 0.191 m, these results correspond to RMSE reductions of 93.4%, 93.0%, and 93.2%, respectively. Thus, explicit rear-to-front propagation of virtual heading commands substantially improved the path-tracking accuracy of the final trailer under identical vehicle and steering constraints.

The values of $|\psi_2|_{\max}$ obtained using BS-RVH were 8.82°, 9.16°, and 5.58° on the S-curve, circular, and figure-eight paths, respectively, which were lower than the corresponding CURV values of 10.06°, 9.73°, and 7.19°. In contrast, $|\psi_1|_{\max}$ was not consistently reduced on every path; for example, on the circular path, BS-RVH and CURV produced 11.53° and 10.38°, respectively. Therefore, the primary advantage of BS-RVH is the improved path-tracking accuracy of the final tracking body and the regulation of the downstream hitch angle, rather than a uniform reduction of every hitch angle.

The local analysis in Section 2.5 shows that, under nonzero longitudinal velocity and bounded desired-command derivatives, the recursive hitch-angle errors are locally ultimately bounded for $K_{\psi_i} > 0$. The terminal-trailer tracking-error dynamics are locally stable for $K_{\text{head}} > 0$ and $K_{\text{ct}} > 0$ in the unsaturated operating region. Moreover, the desired hitch-angle saturation can be interpreted as a bounded residual input to the subsequent recursive stage. For the nominal two-trailer simulations, this saturation was not activated on any curved path; hence, the residual defined in Equation (26) remained zero.

The additional tractor–three-trailer validation in Figure 8 and Table 3 further demonstrates the stage-wise extension of BS-RVH. The controller completed the straight, S-curve, circular, and figure-eight paths without jackknifing. For the curved paths, the lateral RMSE of trailer 3 was 0.085 m, 0.112 m, and 0.073 m, respectively. On the figure-eight path, the maximum hitch angles were 9.46°, 7.42°, and 6.39° for $\psi_1$, $\psi_2$, and $\psi_3$, respectively. The desired hitch-angle saturation was also inactive in these nominal three-trailer validation cases. These results support the scalability of the recursive virtual-heading structure through the addition of one control stage per hitch connection.

The present results should be interpreted within the assumed low-speed kinematic operating conditions, including on-axle hitches, constant reverse velocity, no tire slip, and accurate state measurements. Future work will investigate the effects of steering-actuator dynamics, off-axle hitch geometry, tire slip, state-estimation uncertainty, and longitudinal-velocity variation. Experimental validation using a physical articulated platform will also be considered to evaluate real-time feasibility under practical operating conditions.

## 6. Conclusions

This paper proposed a backstepping-based recursive virtual-heading (BS-RVH) controller for reverse path tracking of multi-trailer systems. The controller converts the lateral and travel-heading errors of the final trailer into a desired heading rate and recursively propagates the resulting virtual-heading commands from the rear trailer toward the tractor. At each hitch stage, a desired hitch angle and the desired heading rate of the preceding body are generated, after which the tractor command is obtained through the Ackermann steering relation.

For the tractor–two-trailer system, BS-RVH achieved lateral RMSE values of 0.015 m, 0.021 m, and 0.013 m on the S-curve, circular, and figure-eight paths, respectively, and completed all paths without jackknifing. Compared with CURV, the proposed controller reduced the lateral RMSE by more than 93% on all three curved paths. On the figure-eight path, BS-RVH reduced the lateral RMSE from 0.191 m to 0.013 m and reduced $|\psi_2|_{\max}$ from 7.19° to 5.58°.

A local boundedness analysis was provided for the recursive hitch-angle errors and terminal-trailer tracking loop under the nominal kinematic assumptions. The analysis also characterized desired hitch-angle saturation as a bounded residual acting on the recursive stages. For the reported nominal simulations, the saturation residual was zero, indicating that the generated virtual-heading commands remained within the prescribed feasible hitch-angle range.

The recursive structure was further validated using a tractor–three-trailer system. BS-RVH completed the straight, S-curve, circular, and figure-eight paths without jackknifing, and the trailer 3 RMSE remained below 0.12 m on all curved paths. These results demonstrate that the proposed framework can be extended stage by stage to additional passive trailers while maintaining bounded articulation in the evaluated nominal scenarios.

Future work will extend the validation to dynamic vehicle models and experimental platforms, with particular emphasis on tire slip, actuator dynamics, sensor uncertainty, off-axle hitches, and robustness under speed variation.

**Author Contributions:** Conceptualization, H.S. and M.K.; methodology, H.S. and J.K.; software, H.S. and J.K.; validation, H.S. and M.K.; formal analysis, H.S., J.K. and H.M.; investigation, H.S. and M.K.; resources, H.S. and J.K.; data curation, H.S. and M.K.; writing—original draft preparation, H.S. and J.K.; writing—review and editing, H.S., M.K., H.M. and J.K.; visualization, H.S. and M.K.; supervision, J.K.; project administration, H.S. and J.K.; funding acquisition, H.S. and H.M. All authors have read and agreed to the published version of the manuscript.

**Funding:** This research was supported by the Regional Innovation System & Education (RISE) program through the Chungbuk Regional Innovation System & Education Center, funded by the Ministry of Education (MOE) and Chungcheongbuk-do, Republic of Korea (grant number 2026-RISE-11-013-03). This research was supported by the "Advanced GPU Utilization Support Program," funded by the Government of the Republic of Korea through the Ministry of Science and ICT (MSIT); and the Information Technology Research Center (ITRC) support program (grant number IITP-2026-RS-2024-00437494), funded by MSIT and supervised by the Institute for Information & Communications Technology Planning & Evaluation (IITP).

**Institutional Review Board Statement:** Not applicable.

**Informed Consent Statement:** Not applicable.

**Data Availability Statement:** The simulation data and source code supporting the findings of this study are available from the corresponding author upon reasonable request.

**Conflicts of Interest:** The authors declare no conflicts of interest.

## Abbreviations

The following abbreviations are used in this manuscript:

| | |
|---|---|
| BS-RVH | Backstepping-Based Recursive Virtual-Heading |
| CURV | Curvature-Based Two-Stage Controller |
| DSE | Direct Single-Trailer Extension |
| MPC | Model Predictive Control |
| RMSE | Root-Mean-Square Error |

## References


1. Pradalier, C.; Usher, K. A Simple and Efficient Control Scheme to Reverse a Tractor-Trailer System on a Trajectory. In Proceedings of the IEEE International Conference on Robotics and Automation, Rome, Italy, 10–14 April 2007; pp. 2208–2214.
2. Leng, Z.; Minor, M. A Simple Tractor-Trailer Backing Control Law for Path Following. In Proceedings of the IEEE/RSJ International Conference on Intelligent Robots and Systems, Taipei, Taiwan, 18–22 October 2010; pp. 5538–5542.
3. Murillo, M.; Sánchez, G.; Deniz, N.; Genzelis, L.; Giovanini, L. Improving Path-Tracking Performance of an Articulated Tractor-Trailer System Using a Non-Linear Kinematic Model. *Comput. Electron. Agric.* **2022**, *196*, 106826. [CrossRef]
4. Bin Salamah, Y. Sliding Mode Controller for Autonomous Tractor-Trailer Vehicle Reverse Path Tracking. *Appl. Sci.* **2023**, *13*, 11998. [CrossRef]
5. Robat, A.B.; Arezoo, K.; Alipour, K.; Tarvirdizadeh, B. Dynamics Modeling and Path Following Controller of Tractor-Trailer-Wheeled Robots Considering Wheels Slip. *ISA Trans.* **2024**, *148*, 45–63. [CrossRef] [PubMed]
6. Shin, H.; Kim, M.-J.; Baek, S.; Crane, C.D.; Kim, J. Perpendicular Parking Path Generation and Optimal Path Tracking Algorithm for Auto-Parking of Trailers. *Int. J. Control Autom. Syst.* **2022**, *20*, 3006–3018. [CrossRef]
7. Hu, Z.; Ma, R. Adaptive Event-Triggered Tracking Control via Switching Functions. *Automatica* **2026**, *185*, 112813. [CrossRef]
8. Hu, Z.; Ma, R.; Zhang, S.; Wang, H.; Liu, X.; Zhao, D. Resilient Memory-Event-Triggered Predictive Tracking Control for Unmanned Ground Vehicle. *IEEE Trans. Intell. Veh.* **2026**, *11*, 500–510. [CrossRef]
9. Cheng, J.; Wang, B.; Zhang, Y.; Wang, Z. Backward Orientation Tracking Control of Mobile Robot with N Trailers. *Int. J. Control. Autom. Syst.* **2017**, *15*, 867–874. [CrossRef]
10. Kolb, J.; Nitzsche, G.; Wagner, S.; Röbenack, K. On the Backward Path Tracking Control of N-Trailer Systems. *Syst. Theory Control Comput. J.* **2021**, *1*, 13–20. [CrossRef]
11. Lukassek, M.; Völz, A.; Szabó, T.; Graichen, K. Model Predictive Path-Following Control for General N-Trailer Systems with an Arbitrary Guidance Point. In Proceedings of the 2021 European Control Conference, Delft, The Netherlands, 29 June–2 July 2021; pp. 1335–1340. [CrossRef]
12. Bertolani, D.N.; Bacheti, V.P.; Brandão, A.S.; Carelli, R.; Sarcinelli-Filho, M. Controlling a Multi-Articulated Robot in Backward Movement Using an Adaptive Controller. *Mechatronics* **2023**, *92*, 102967. [CrossRef]
13. Bertolani, D.N.; Bacheti, V.P.; Sarcinelli-Filho, M. Null Space-Based Control with Gain Modulation Applied to a Multi-Articulated Robotic Vehicle in Backward Movement. *ISA Trans.* **2024**, *152*, 487–498. [CrossRef] [PubMed]
14. Morales, J.; Mandow, A.; Martínez, J.L.; Reina, A.J.; García-Cerezo, A. Driver Assistance System for Passive Multi-Trailer Vehicles with Haptic Steering Limitations on the Leading Unit. *Sensors* **2013**, *13*, 4485–4498. [CrossRef] [PubMed]
15. Zhao, T.; Huang, W.; Xu, P.; Zhang, W.; Li, P.; Zhao, Y. A Simple Curvature-Based Backward Path-Tracking Control for a Mobile Robot with N On-Axle Trailers. *Actuators* **2024**, *13*, 237. [CrossRef]
16. Rigatos, G.G.; Busawon, K.K.; Abbaszadeh, M. A Nonlinear Optimal Control Approach for the Truck and N-Trailer Robotic System. *IFAC J. Syst. Control* **2022**, *20*, 100191. [CrossRef]
17. Guevara, L.; Jorquera, F.; Walas, K.; Auat Cheein, F. Robust Control Strategy for Generalized N-Trailer Vehicles Based on a Dual-Stage Disturbance Observer. *Control Eng. Pract.* **2023**, *131*, 105382. [CrossRef]
18. Deniz, N.; Jorquera, F.; Torres-Torriti, M.; Auat Cheein, F. Model Predictive Path-Following Controller for Generalised N-Trailer Vehicles with Noisy Sensors and Disturbances. *Control Eng. Pract.* **2024**, *142*, 105747. [CrossRef]
19. Lukassek, M.; Dahlmann, J.; Völz, A.; Graichen, K. Model Predictive Path-Following Control for Truck–Trailer Systems with Specific Guidance Points—Design and Experimental Validation. *Mechatronics* **2024**, *100*, 103190. [CrossRef]